Journal of Hepatocellular Carcinoma

Dovepress
Taylor & Francis Group

Open Access Full Text Article

ORIGINAL RESEARCH

Establishing a Survival Time Prediction Model for Patients with Hepatocellular Carcinoma After TACE Based on CT Radiomics: A Multi-Center Study

Han Yang[1,*], Juan Zhao[2,*], Yingwei Wang[3], Diwen Zhu[1], Junpeng Gu[1], Weixin Ren[1]

[1]Department of Interventional Radiology, The First Affiliated Hospital of Xinjiang Medical University (Xinjiang Interventional Medicine Clinical Research Center), Xinjiang, Urumqi, 830054, People's Republic of China; [2]Department of Anesthesiology, Sichuan Cancer Hospital & Institute (Sichuan Cancer Center, or Cancer Hospital Affiliated to University of Electronic Scienceand Technology of China), Sichuan, Chengdu, 610041, People's Republic of China; [3]Department of Radiology, The First Affiliated Hospital of Southwest Medical University, Sichuan, Luzhou, 646000, People's Republic of China

*These authors contributed equally to this work

Correspondence: Weixin Ren, Department of Interventional Radiology, The First Affiliated Hospital of Xinjiang Medical University, No. 137 South Li Yu Shan Street, Xinjiang, Urumqi, 830054, People's Republic of China, Tel +86 18011425277, Email rwx1031@163.com

Purpose: This research constructs a prognostic model for overall survival (OS) in hepatocellular carcinoma (HCC) patients using radiomic features from non-contrast CT scans obtained within 24 hours after transarterial chemoembolization (TACE).

Patients and Methods: Patients were retrospectively enrolled from three institutions to form training (n = 112) and validation (n = 56) cohorts from January 2016 to December 2023. All patients underwent a minimum of three TACE treatment sessions. January 2019 served as the cutoff point for dividing the dataset into training and validation cohorts. Univariate and multivariate Cox regression analyses were employed to obtain clinical variables related to OS for constructing the clinical model. The least absolute shrinkage and selection operator (LASSO) and multivariate Cox regression analyses were employed to construct the radiomics model from lipiodol deposits in the target lesions (TL) within 24 hours after the initial TACE, and the clinical-radiomics model was further constructed. Model prediction performance was subsequently assessed by the area under the time-dependent receiver operating characteristic curve (AUC) and calibration curve. Additionally, Kaplan-Meier analysis was used to evaluate the model's value in predicting OS.

Results: The clinical-radiomics model predicted OS at 1, 2, and 3 years more accurately than the clinical or radiomics model alone (training group, AUC = 0.787, 0.765 and 0.827, respectively; validation group, AUC = 0.731, 0.713 and 0.798, respectively). The predicted high-risk subgroup based on the clinical-radiomics model had shorter mOS than predicted low-risk subgroup (training group, 16 m vs 37 m, p = 0.0002; validation group 14 m vs 35 m, p<0.0001), enabling risk stratification of various clinical subgroups.

Conclusion: The radiomic signature derived from lipiodol within 24 hours post-TACE functions as a prognostic biomarker for OS in HCC patients. The clinical-radiomics model demonstrates robust predictive performance, providing a valuable tool for prognostic evaluation in HCC.

Keywords: hepatocellular carcinoma, radiomics, transcatheter arterial chemoembolization, tomography, x-ray computed, overall survival

Introduction

Hepatocellular carcinoma (HCC) accounts for approximately 75–85% of primary liver cancers, and its incidence has steadily increased over the past two decades, now ranking as the third leading cause of cancer-related mortality worldwide.[1] Transarterial chemoembolization (TACE) is a minimally invasive procedure recognized for its significant efficacy and low complication rates. It effectively reduces tumor burden and is widely considered the first-line treatment for localized, advanced HCC.[2] Recent years have seen significant advancements in liver cancer treatment using TACE, including the introduction of drug-eluting beads and radioembolization, coupled with the implementation of "precision TACE", leading to encouraging results. However, not all patients benefit equally from multiple TACE

Received: 20 April 2025
Accepted: 19 September 2025
Published: 7 October 2025

sessions, and there is considerable variability in survival outcomes post-TACE, particularly in long-term efficacy. Notably, substantial heterogeneity exists in overall survival (OS) times among different patients, underscoring the need for more personalized treatment strategies.[3–5] Consequently, it is clinically imperative to accurately evaluate therapeutic responses following TACE in patients with HCC. Such assessments are crucial for devising optimal treatment strategies, advancing precision medicine, and ultimately improving patient survival outcomes. The six-and-twelve model based on general image information (equal to the maximum diameter (cm) of the tumor plus the number of tumors) was developed recently, and its accuracy in predicting the effectiveness of TACE using survival probability was 70–75%,[6] which was recommended as a pre-TACE expected survival model in the 2020 Chinese Society of Clinical Oncology (CSCO) guidelines.

Radiomics, a rapidly evolving field, enables the extraction of high-throughput quantitative features from medical imaging data. These features encapsulate a wealth of foundational information related to the tumor's genetic and molecular profile,[7] thereby providing a comprehensive reflection of tumor heterogeneity and biological behavior. This approach holds significant potential for predicting patient prognosis and guiding personalized therapeutic interventions. Numerous recent studies have confirmed that computed tomography (CT) radiomics can differentiate liver cancers of different molecular pathological types,[8] assist in clinical decision-making, and improve patient prognosis.[9–11] Furthermore, research[12] has demonstrated that the lipiodol accumulation patterns within the target lesion (TL) can effectively assess tumor responsiveness after TACE, but there have been no reports on radiomic studies related to lipiodol deposits within the TL. Therefore, this study establishes a prognostic model that incorporates both lipiodol-retention radiomics after TACE and clinical features. This model can guide clinicians in choosing the most effective treatment plan and provide more accurate and personalized treatment decisions for liver cancer patients.

Materials and Methods

Patients

This study was approved by the institutional review board of the First Affiliated Hospital of Xinjiang Medical University (No. K202502-16). The need for written informed consent was waived due to the retrospective study design. All the clinical data were collected and reviewed confidentially from the hospital's electronic database. All procedures involving human participants were conducted in accordance with the Declaration of Helsinki.

Clinical and imaging data were retrospectively collected from patients diagnosed with HCC who underwent TACE at three hospitals between January 2016 and December 2023. A total of 168 patients meeting the inclusion criteria were enrolled and stratified into a training cohort (n = 112) and a validation cohort (n = 56), with January 2019 serving as the cutoff for cohort allocation. Given the limitations in patient enrollment numbers for this study, and in accordance with relevant literature on prognostic prediction model development and validation,[13] we did not partition an external validation cohort for the prediction model. Inclusion criteria encompassed: (a) confirmation by histopathology or adherence to the HCC diagnosis criteria of the European Association for the Study of the Liver;[14] (b) age range of 18–75 years with a KPS score exceeding 75; (c) Barcelona Clinic Liver Cancer (BCLC) staging of A/B and liver function classified as Child-Pugh A/B; (d) receipt of at least three consecutive TACE treatments in the same liver segment, in accordance with the Expert Consensus of the Chinese College of Interventionalists;[15] (e) CT scan within 24 hours post-initial TACE; (f) complete clinical data availability. Exclusion criteria comprised: (a) TACE treatments in different liver segments; (b) interval exceeding 6 months between first and last TACE; (c) TL treated with alternative methods prior to TACE (including targeted drug therapy, radiotherapy, surgical interventions, etc).; (d) Combined with other malignant tumor (e) incomplete clinical or imaging data; (f) image quality insufficient for region of interest (ROI) segmentation; (g) presence of severe portal vein tumor thrombus or extrahepatic metastasis; (h) TACE without use of lipiodol. The patient selection process is illustrated in Figure 1. The workflow chart of necessary steps is presented in Figure 2.

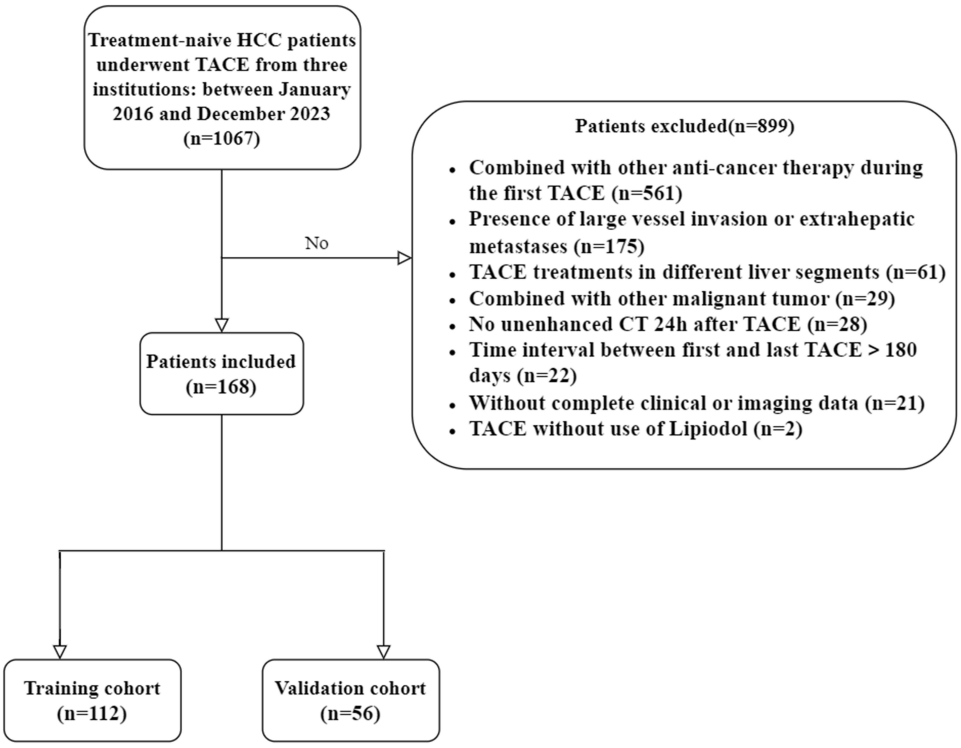

Figure 1 Flowchart shows recruitment pathway for patients.

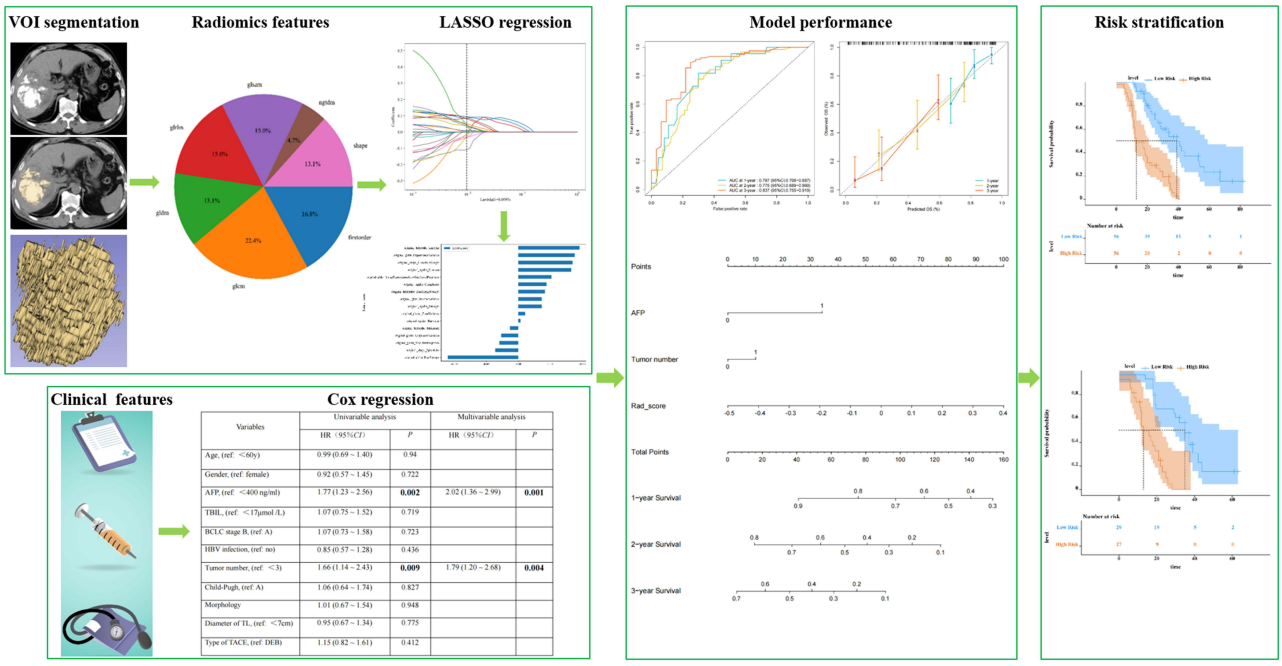

Figure 2 The workflow chart of necessary steps of this study.

CT Protocol

CT images were acquired with multi-row spiral CT scanners (GE DISCOVERY CT 750; UNITED CT 960; CANON AQUILION ONE Genesis CT 320) at three centers. The scanner utilized a tube voltage of 120 kV with automatic tube current modulation, and the reconstruction thickness was set to 5.0 mm. Abdominal scans were performed with non-contrast

https://doi.org/10.2147/JHC.S535606

and triple-phase contrast enhancement. The contrast agent was administered via the arm vein at a rate of 3.0 mL/s, with a dosage of 1.5 mL per kilogram of body weight. The arterial phase, portal venous phase, and delayed phase scans were carried out at 25–30 seconds, 60 seconds, and 90–120 seconds, respectively. All patients were instructed to fast for 4–6 hours prior to the examination and were required to hold their breath during the scanning process. The detailed parameters for each CT scanners are listed in Supplementary Data S1.

TACE Procedure

Following routine disinfection, draping, and anesthesia administration, the right femoral artery was punctured, and a hepatic catheter was inserted to perform abdominal trunk and hepatic arteriography. The TACE procedures were conducted by experienced senior physicians with over 10 years of expertise in interventional therapy. Throughout the procedure, continuous monitoring of ECG and oxygen saturation is maintained. Post-procedure, the catheter is extracted, the sheath is removed, and the puncture site is compressed and dressed. All enrolled patients received conventional transarterial chemoembolization (C-TACE) as their initial treatment. Among them, 19.6% (33/168) underwent drug-eluting beads transarterial chemoembolization (DEB-TACE) in at least one TACE session. The TACE procedure is detailed in Supplementary Data S2.

Lesions Segmentation and Conventional CT Evaluation

Using the 3D Slicer (version 5.4.0, https://www.slicer.org/), the volume of interest (VOI) was threshold-delineated on the lipiodol deposits of TL on non-contrast CT images, layer by layer, by a radiologist (Physician A) with 7 years of diagnostic abdominal imaging experience, preserving the ambiguous boundaries (Figure 3). To evaluate inter-observer agreement, 40 cases were randomly selected, and an additional deputy chief radiologist (Physician B) with over 10 years of expertise in abdominal imaging, along with Physician A, independently performed VOI segmentation. Imaging features evaluated included morphology, tumor number and maximum diameter of TL.

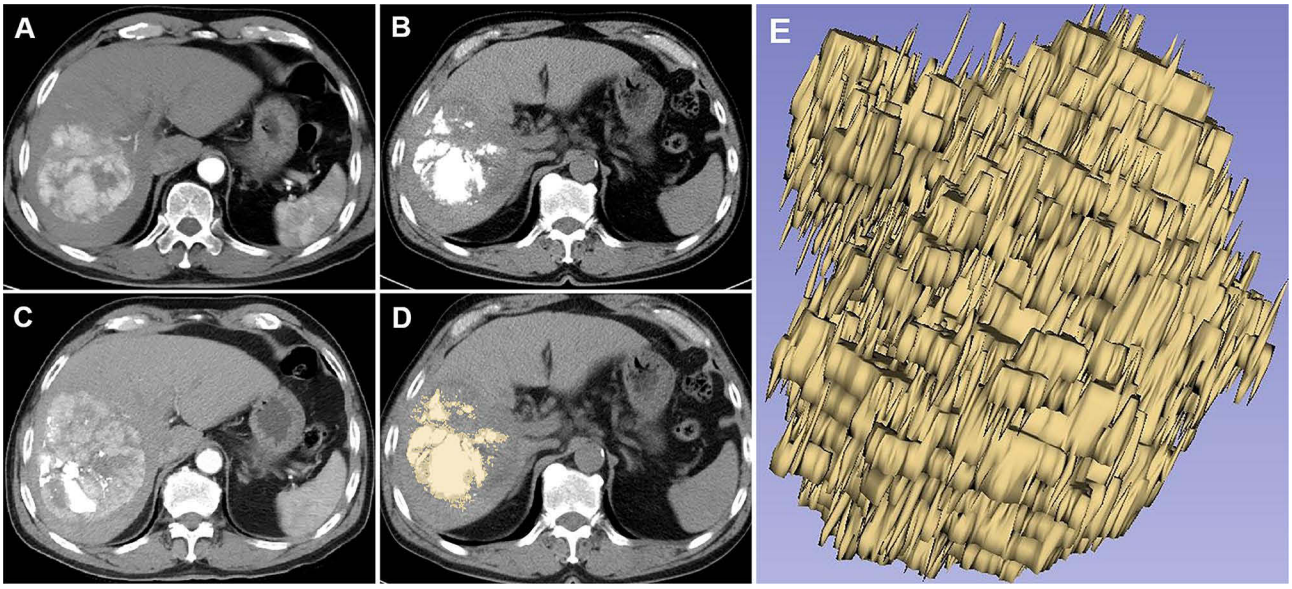

Figure 3 Segmentation of lipiodol in tumor after TACE by using 3D-Slicer software. Baseline axial CT-enhanced arterial-phase image depicting the largest dimension of a tumor in the right hepatic lobe (**A**); Non-contrast CT of the same level within 24 hours after the initial TACE procedure (**B**); Axial CT enhancement following three TACE procedures demonstrating tumor progression from baseline (**C**); Threshold-based segmentation delineating the lipiodol deposits within the TL after the initial TACE procedure, illustrated in a figure corresponding to (**B**). (**D**); Three-dimensional reconstruction of lipiodol deposits within the TL generated through volumetric segmentation across sequential cross-sectional imaging slices (**E**).

Radiomics Feature Extraction

The Pyradiomics package (version 3.0.1), was utilized to standardize CT images from various centers to a uniform voxel size of 1mm × 1mm × 1mm. This process involves discretizing voxel intensity values with a fixed bin width of 25 Hounsfield Units (HU), which serves to mitigate image noise and normalize voxel intensities across the dataset. After image normalization and resampling (1, 1, 1), we extracted seven categories of radiomics features (shape, gray-level cooccurrence matrix (glcm), gray-level run length matrix (glrlm), gray-level size zone matrix (glszm), gray-level dependence matrix (gldm), neighborhood gray-tone difference matrix (ngtdm) and first-order statistics) of each VOI (Figure 4).

Feature Selection and Construction of the Radiomics Signature

Following Z-score normalization, invalid features were eliminated from the dataset, and gaps were filled with mean values. To reduce potentially redundant features and decrease data dimensionality, a three-step procedure was implemented to identify the most predictive radiomics features. First, the intra-class correlation coefficient (ICC) was utilized to evaluate inter-observer reliability, and radiomic features with an ICC of 0.75 or higher, indicating good reproducibility, were selected. Second, redundant features with correlation coefficients exceeding 0.90 were removed based on the Spearman's rank correlation test. Finally, the least absolute shrinkage and selection operator (LASSO) algorithm was employed to select features with higher correlation coefficients and to construct a cox regression model. The penalty term coefficient (λ) was determined through a 10-fold cross-validation iteration to maximize the AUC. Radiomics score ("rad_score") was computed by combining their key features based on LASSO Cox regression coefficient.

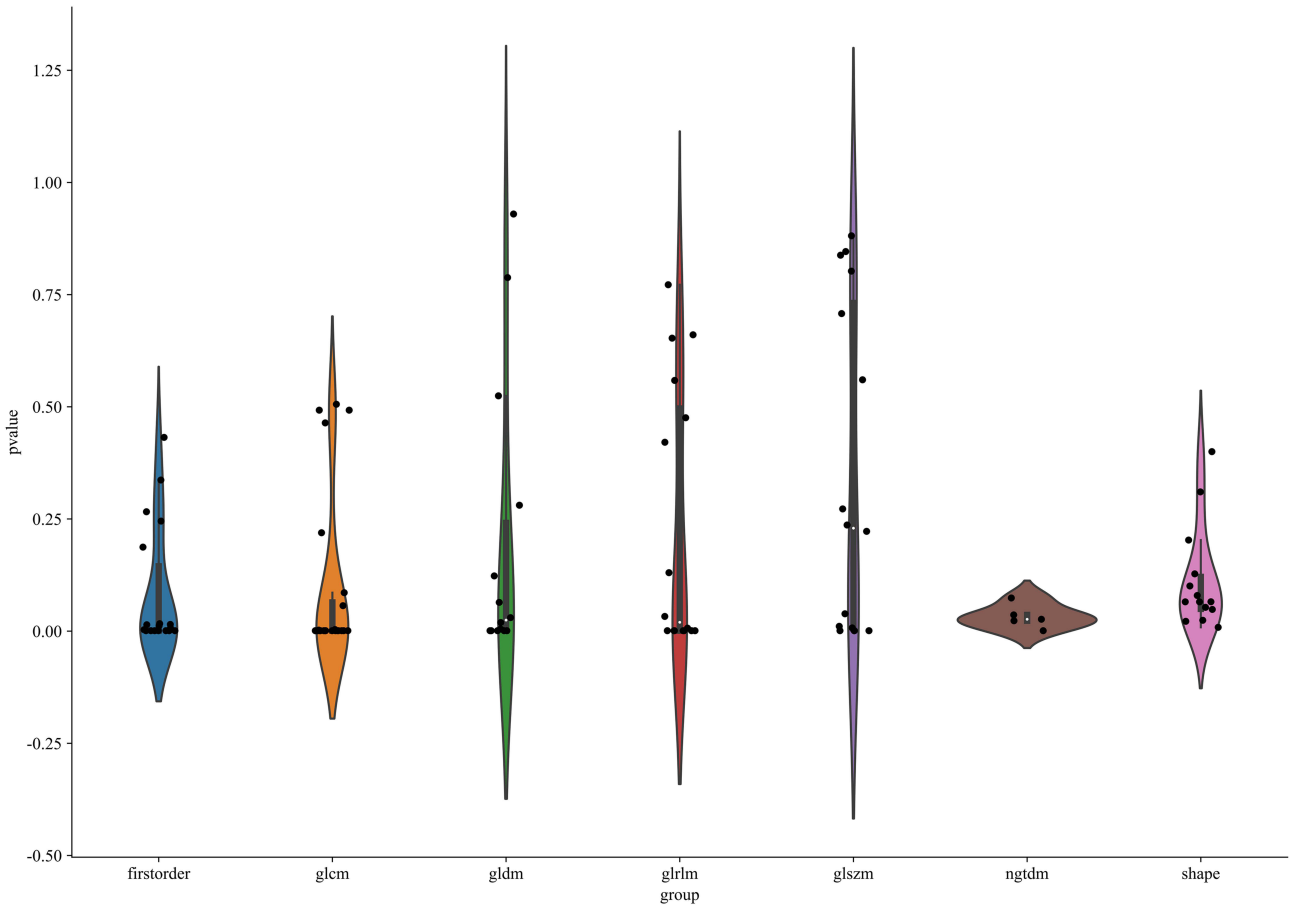

Figure 4 The proportion, distribution and p of various radiomics features.

https://doi.org/10.2147/JHC.S535606

Follow-Up and Efficacy Evaluation

The follow-up protocol consisted of one visit three months after the initial TACE, followed by biannual visits in the second year, and semi-annual to annual visits from the third year onwards. Follow-up assessments included liver function tests, ultrasound examinations, abdominal CT/ magnetic resonance imaging (MRI) scans, and additional necessary laboratory tests. Based on these evaluations, if evidence of residual or new hepatic lesions was observed, TACE treatment was repeated. The study's primary endpoint was OS, defined as the duration from the initiation of TACE treatment to death or the last follow-up. Furthermore, the study recorded each patient's demographic and clinical characteristics, including gender, age, BCLC staging, HbsAg positive expression, serum Tbil, and analyses identified alpha-fetoprotein (AFP) levels.

Statistical Analysis

Statistical analyses were analyzed using SPSS Statistics software (V.26, IBM) and R software (version 4.4.3, http://www.r-project.org). Normally distributed continuous variables are presented as mean ± standard deviation ($\bar{x} \pm s$) and compared using independent samples *t* tests. Non-normally distributed variables are expressed as median and interquartile range M (Q1, Q3), with differences between groups analyzed using the Mann–Whitney *U*-test. Categorical variables are presented as number (%), with group comparisons conducted using the chi-square ($\chi 2$) test. A p-value < 0.05 indicates statistical significance. Survival curves were constructed using Kaplan–Meier and Log rank tests. Cox regression was employed to examine risk factors. Statistical significance was determined at $p < 0.05$.

Results

Baseline Characteristics

Table 1 presents the demographic information and laboratory indicators of the patients. No statistically significant differences were observed between the training and validation cohorts regarding age, gender, etiology, tumor diameter, number of tumors, tumor morphology, BCLC staging, Child-Pugh classification, AFP, total bilirubin and type of TACE (all P values > 0.05).

Table 1 Baseline Characteristics of Training and Validation Cohort

Characteristics	Overall (n = 168)	Training Cohort (n = 112)	Validation Cohort (n = 56)	p	t/Z/χ^2
Gender (%)				0.67	0.20
Male	141 (83.93)	95 (84.82)	46 (82.14)		
Female	27 (16.07)	17 (15.18)	10 (17.86)		
Age (years)	56.06 ± 12.59	56.21 ± 12.17	55.75 ± 13.49	0.82	0.23
AFP				0.65	0.21
<400 ng/mL	109 (64.88)	74 (66.07)	35 (62.50)		
≥400 ng/mL	59 (35.12)	38 (33.93)	21 (37.50)		
TBIL				0.50	0.46
<17 μmol /L	105 (62.50)	68 (60.71)	37 (66.07)		
≥17 μmol /L	63 (37.50)	44 (39.29)	19 (33.93)		
HBV infection				0.70	0.15
No	39 (23.21)	25 (22.32)	14 (25.0)		
Yes	129 (76.79)	87 (77.68)	42 (75.0)		

(*Continued*)

Table 1 (Continued).

Characteristics	Overall (n = 168)	Training Cohort (n = 112)	Validation Cohort (n = 56)	p	t/Z/χ^2
Diameter (cm) of TL	4.9 (4.2, 5.5)	4.9 (4.2, 5.3)	5.0 (4.1, 6.3)	0.26	−1.14
Tumor number				0.64	0.22
<3	55 (32.73)	38 (33.93)	17 (30.36)		
≥3	113 (67.26)	74 (66.07)	39 (69.64)		
Morphology				0.94	0.13
Circular/quasi-circular	96 (57.14)	65 (58.04)	31 (55.36)		
Irregularity	44 (26.19)	29 (25.89)	15 (26.78)		
Peritumoral enhancement	28 (16.67)	18 (16.07)	10 (17.86)		
BCLC				0.55	0.36
A	49 (29.17)	31 (27.68)	18 (32.14)		
B	119 (70.83)	81 (72.32)	38 (67.86)		
Child-Pugh				0.75	0.10
A	145 (86.31)	96 (85.71)	49 (87.5)		
B	23 (13.69)	16 (14.29)	7 (12.5)		
Type of TACE				0.68	0.17
C-TACE	135 (80.36)	89 (79.46)	46 (82.14)		
DEB-TACE	33 (19.64)	23 (20.54)	10 (17.86)		

Abbreviations: AFP, alpha-fetoprotein; TBIL, total bilirubin; HBV, hepatitis B virus; TL, target lesions; BCLC, stage of Barcelona Clinic Liver Cancer; C-TACE, conventional transarterial chemoembolization; DEB-TACE, drug-eluting beads transarterial chemoembolization.

Radiomics Feature Analysis and Rad_score Calculation

A total of 107 features were extracted from each VOI. First, radiomics features with ICC<0.75 were excluded. Then, predictors with a Spearman correlation coefficient > 0.9 were excluded to select independent predictive features (Supplementary Data S3). Subsequently, LASSO regression analysis identified the robust radiomics features (Figure 5A and B). 16 robust radiomics features are presented in Figure 6 and Supplementary Data S4. The Rad_score is calculated by multiplying each feature by its respective coefficient and subsequently summing these weighted values.

Modeling and Evaluation of Radiomics Nomogram

Univariate analysis revealed that AFP (P=0.002) and tumor number (P=0.009) were significantly associated with OS following TACE (P < 0.05). A Cox multivariate model, adjusting for factors identified in the univariate analysis, indicated that AFP >400 ng/mL [P=0.001; Hazard Ratio (HR): 2.02, 95% confidence interval (CI): 1.36–2.99], and tumor number (n>3) [P=0.004; HR: 1.79, 95% CI: 1.20–2.68] are independent risk factors influencing OS (Table 2). Compared to the clinical and radiomics models, the clinical-radiomics model demonstrated superior predictive performance, with an AUC for 1, 2, and 3 years OS of 0.787 (0.698–0.877), 0.765 (0.679–0.850), 0.827 (0.745–0.909) in the training group, respectively, and 0.731 (0.591–0.871), 0.713 (0.528–0.898), 0.798 (0.660–0.927) in the validation group, respectively (Figure 7A and B). AFP, tumor number, along with and without the rad-score, were included in the clinical model and the clinical-radiomics model, which were finally displayed through nomograms (Figure 7C). The calibration curves indicated well calibrated between model-predicted and observed probability of OS (Figure 7D and E). For

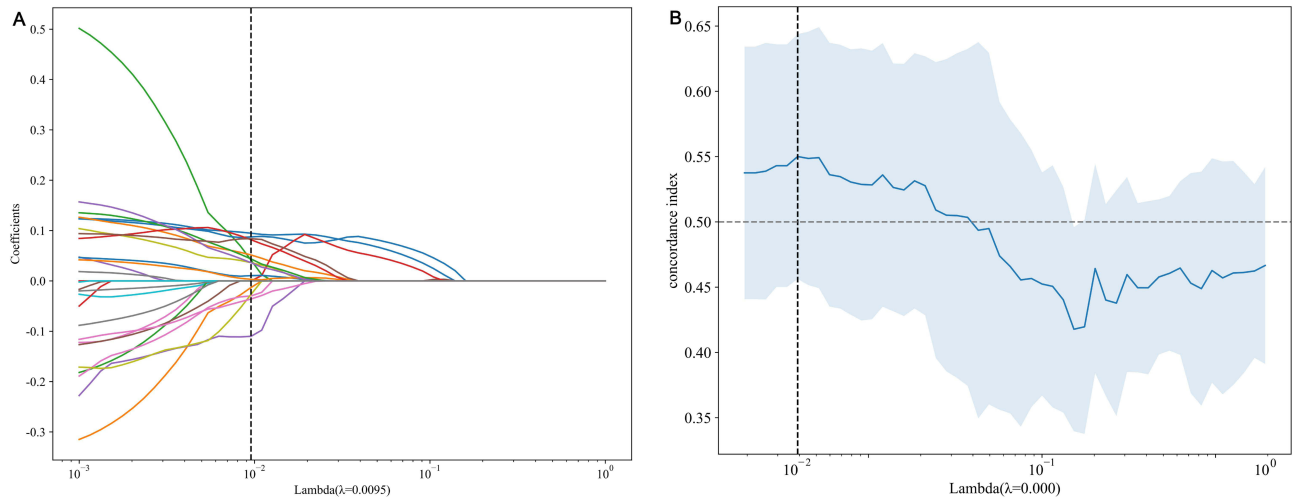

Figure 5 LASSO plots for feature screening generated using Python. Lambda on the horizontal axis and coefficients on the vertical axis (**A**). Lambda on the horizontal axis and mean square error (MSE) on the vertical axis (**B**).

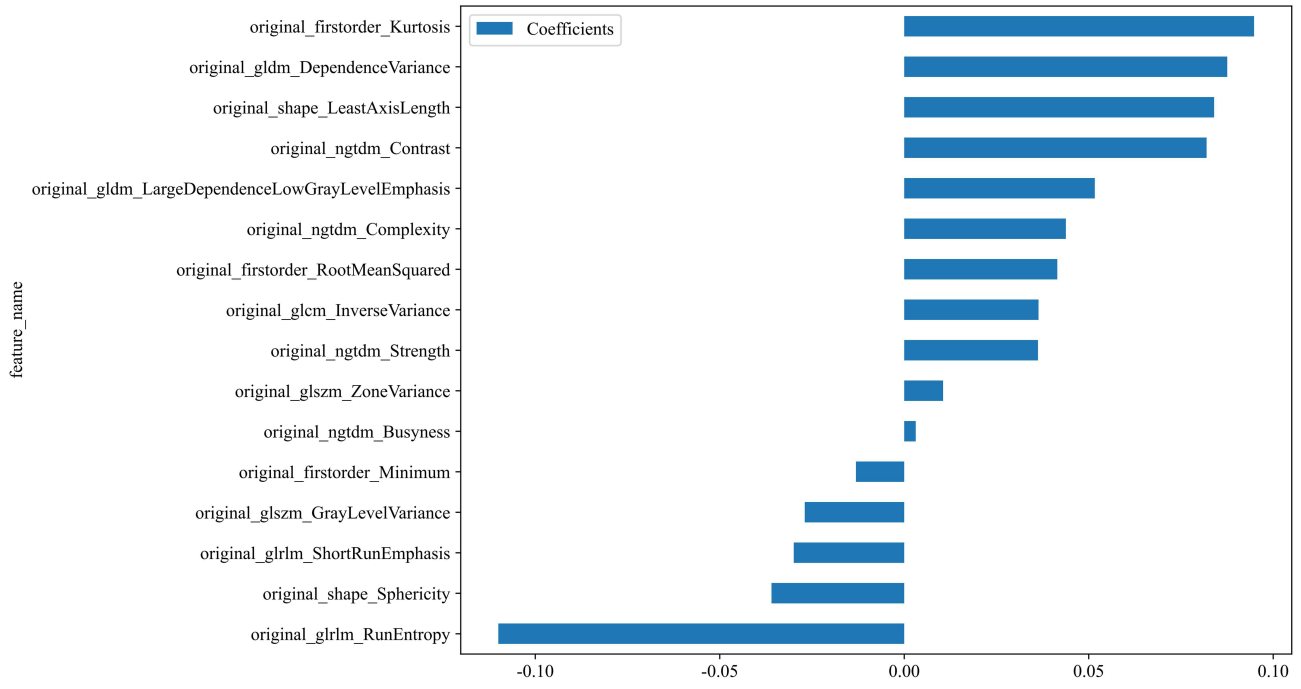

Figure 6 Weighting coefficients of 16 robust radiomics features.

predicting OS in HCC patients receiving TACE treatment, the clinical-radiomics model achieved a C-index of 0.72 (95% CI: 0.65–0.76) in the training cohort and 0.68 (95% CI: 0.58–0.79) in the validation cohort, surpassing the Six-and-twelve model, with C-indexes of 0.67 (95% CI: 0.61–0.72) for training and 0.64 (95% CI: 0.53–0.74) for validation cohort (Figure 8A and B).

Survival Analysis

By the end of the follow-up period, among the 168 patients, 130 (77.38%) had either died or were lost to follow-up, while 38 (22.62%) remained alive, with a median survival time of 25.0 months (95% CI: 19.8–30.2). The difference in lipiodol dosage during initial embolization has no statistically significant effect on patient survival time (Supplementary Data S5). The

Table 2 Cox Regression Analysis of Clinical Variables for Predicting Survival

Variables	Univariable Analysis		Multivariable Analysis	
	HR (95% CI)	*P*	HR (95% CI)	*P*
Age, (ref: <60y)	0.99 (0.69 ~ 1.40)	0.94		
Gender, (ref: female)	0.92 (0.57 ~ 1.45)	0.722		
AFP, (ref: <400 ng/mL)	1.77 (1.23 ~ 2.56)	**0.002**	2.02 (1.36 ~ 2.99)	**0.001**
TBIL, (ref: <17μmol /L)	1.07 (0.75 ~ 1.52)	0.719		
BCLC stage B, (ref: A)	1.07 (0.73 ~ 1.58)	0.723		
HBV infection, (ref: no)	0.85 (0.57 ~ 1.28)	0.436		
Tumor number, (ref: <3)	1.66 (1.14 ~ 2.43)	**0.009**	1.79 (1.20 ~ 2.68)	**0.004**
Child-Pugh, (ref: A)	1.06 (0.64 ~ 1.74)	0.827		
Morphology	1.01 (0.67 ~ 1.54)	0.948		
Diameter of TL, (ref: <7cm)	0.95 (0.67 ~ 1.34)	0.775		
Type of TACE, (ref: DEB)	1.15 (0.82 ~ 1.61)	0.412		

Note: P value of bold text indicates statistically significant.
Abbreviations: AFP, alpha-fetoprotein; TBIL, total bilirubin; BCLC, stage of Barcelona Clinic Liver Cancer; HBV, hepatitis B virus; TL, target lesions; TACE, transarterial chemoembolization.

median predicted value of the clinical-radiomic model score served as the threshold to categorize patients into high-risk and low-risk groups. In the training cohort, the median survival time for high-risk patients was 16.0 months (95% CI: 11.3–20.7), whereas for low-risk patients it was 37.0 months (95% CI: 31.5–42.5), with the low-risk group demonstrating significantly longer survival times (P = 0.0002). Similarly, in the validation cohort, the median survival time for high-risk patients was 14.0 months (95% CI: 9.2–18.8), and for low-risk patients, 35.0 months (95% CI: 28.7–41.3), with the low-risk group again exhibiting significantly better survival times (P<0.0001), as illustrated in Figure 9A and B.

Discussion

TACE has been established as the recommended treatment for BCLC stage B HCC patients.[16] However, due to the significant heterogeneity in the biological behavior of liver cancer cells, previous studies[17] have demonstrated that the recurrence rate remains above 70% even five years post-TACE treatment. Identifying an accurate and effective method to predict tumor response following TACE and the survival duration of HCC patients is a crucial objective in achieving precise, personalized medical care.

The widespread application of artificial intelligence in the medical field has led to an increasing number of interventional radiologists utilizing radiomics to predict tumor response in HCC patients after TACE treatment. Kong et al[18] conducted a retrospective study involving 99 HCC patients, establishing clinical, radiomic, and combined models based on preoperative T2WI-weighted images and clinical data. Their findings demonstrated that the radiomic model effectively differentiated tumor response in HCC patients post-TACE, achieving an area AUC of 0.812 in the training cohort and 0.866 in the validation cohort. Moreover, the incorporation of clinical data into the combined model enhanced its predictive performance (AUC = 0.861 in the training cohort and AUC = 0.884 in the validation cohort). In a separate study, Cheng et al[7] retrospectively analyzed 100 HCC patients with portal vein tumor thrombus from two centers, all of whom underwent drug-eluting bead transarterial chemoembolization (DEB-TACE). They developed a predictive model by extracting radiomic features from preoperative CT non-contrast and enhanced images, utilizing radiomics combined with machine learning methods. Their results confirmed that the type of portal vein tumor thrombus and the number of tumors are independent risk factors affecting OS in patients. Furthermore, both the radiomic model and the combined model exhibited significant differences in the integrated discrimination index for predicting 12-month OS in HCC patients.

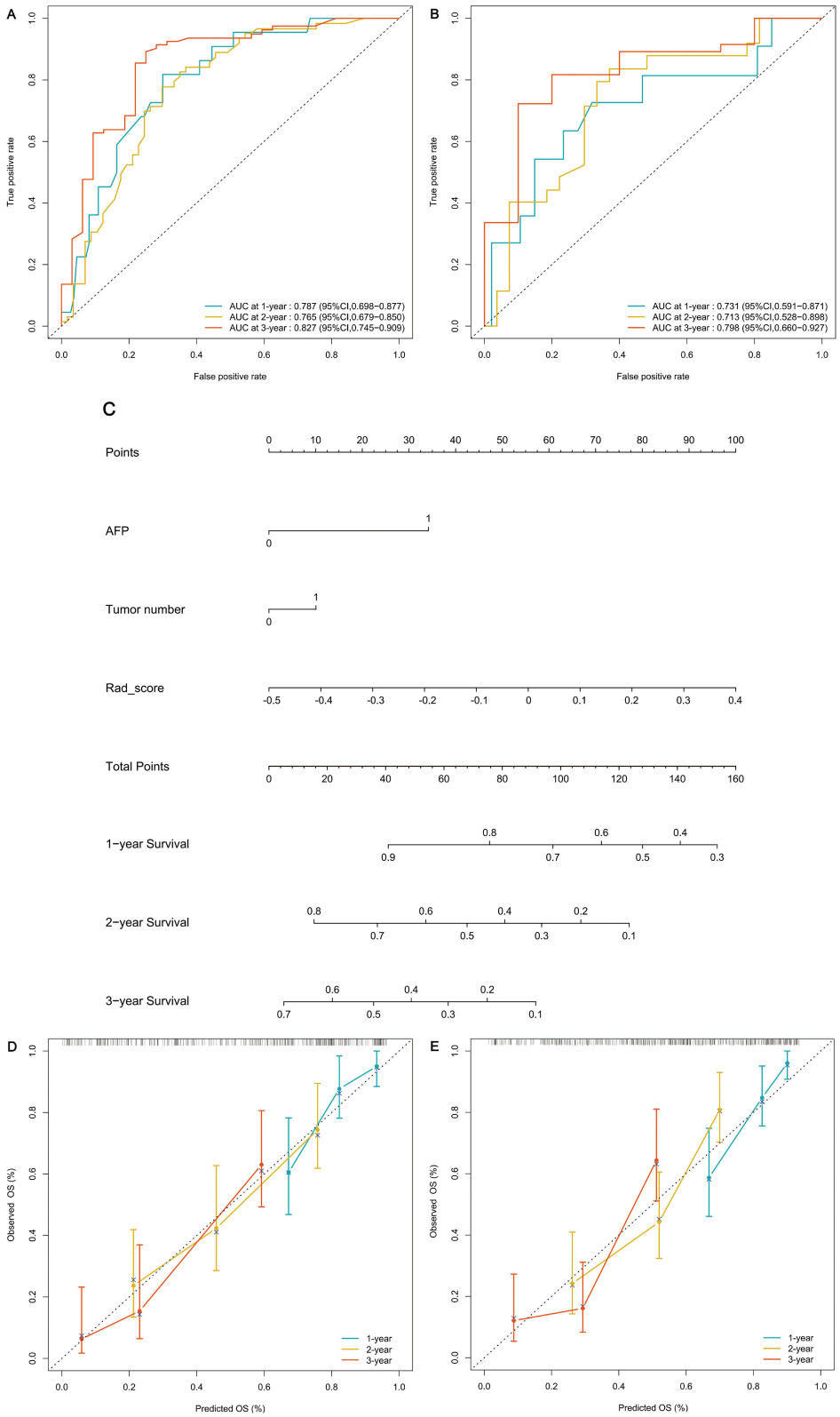

Figure 7 Nomogram, time-dependent ROC curves and calibration curves. Time-dependent receiver operating characteristic curves for predicting 1-year, 2-year, and 3-year OS in the training group (**A**) and validation group (**B**). Clinical-radiomics nomogram (**C**). The calibration curves of clinical-radiomics nomogram in the training group (**D**) and validation group (**E**).

Abbreviations: Rad-score, radiomics score; AUC, area under the curve.

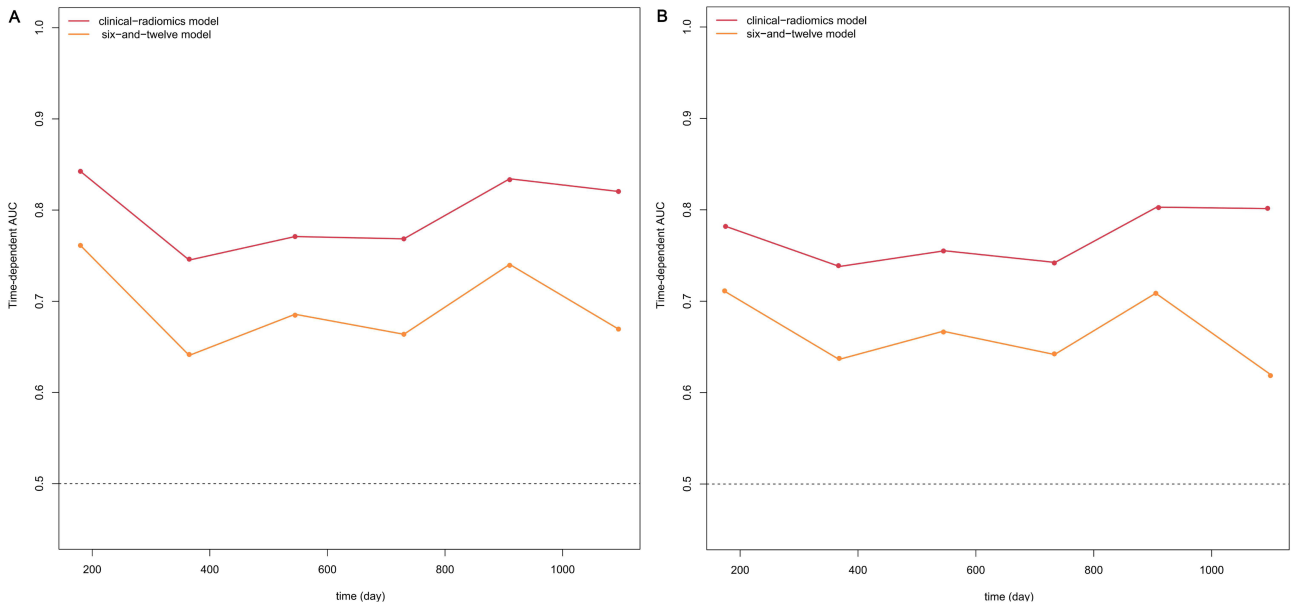

Figure 8 Time-dependent receiver operating characteristic curves of clinical-radiomics model (**A**) and six-and-twelve model (**B**).

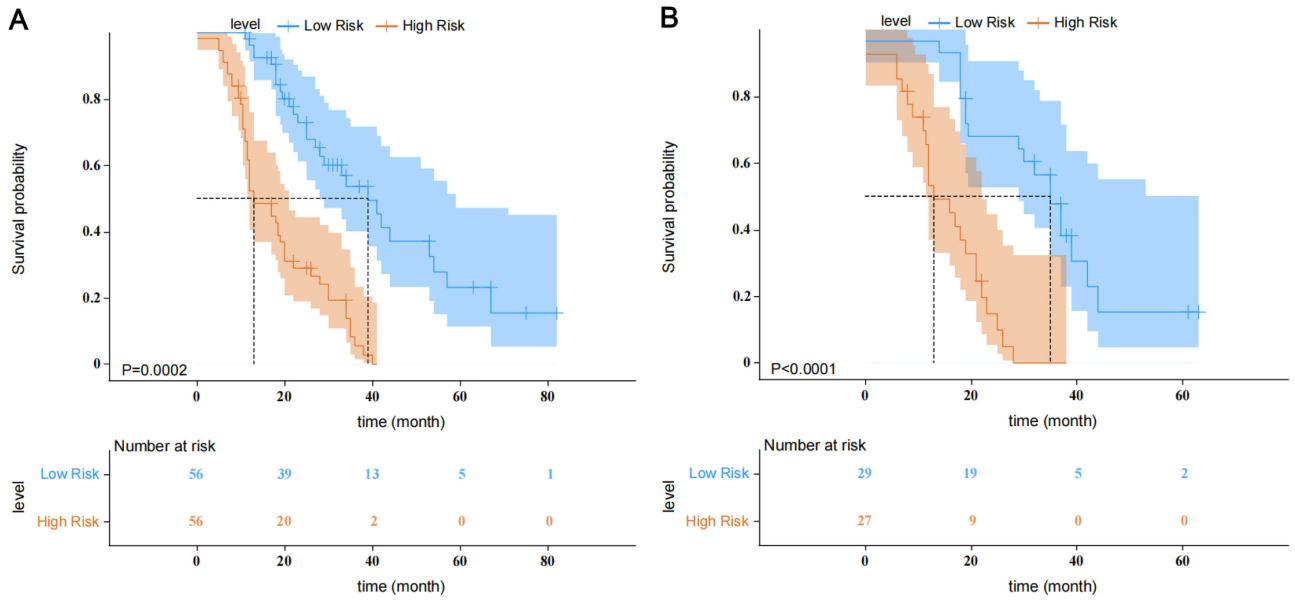

Figure 9 Kaplan-Meier analysis of the prediction performance of the clinical-radiomics model in predicting OS of patients in the training cohort (**A**) and validation cohort (**B**).

The aforementioned studies demonstrate that radiomics can effectively differentiate tumor responses in HCC patients after TACE, and when combined with clinical features, it can further assess patient prognosis and survival duration. A key limitation of these studies is that radiomic models, based on pre-TACE imaging features, do not account for microenvironmental changes in hepatocellular carcinoma occurring after TACE. Chen et al[19] followed up with 101 HCC patients who underwent TACE treatment. Their comparative analysis revealed that the group with good blood supply and good lipiodol-retention (n=59) had significantly higher OS and progression-free survival compared to the group with good blood supply but poor lipiodol-retention (n=42). This study confirmed that the lipiodol-retention patterns within the TL can serve as a direct indicator of tumor necrosis. Miszczuk et al[12] conducted a prospective study on 39 patients with liver tumors, including 22 with HCC and 17 with other types of liver tumors. They collected CT, MRI, and PET-CT

https://doi.org/10.2147/JHC.S535606

images from all patients at 30 days before C-TACE, 1-day, 1-month, 90 days, and 180 days after C-TACE. Based on the quantitative results from the 24-hour postoperative CT follow-up, the lipiodol/ target tumor coverage ratio was significantly higher in HCC patients who responded to TACE compared to those who did not (P=0.004). No significant differences were observed in non-HCC patients. This suggests that lipiodol-retention patterns and its longitudinal clearance status are closely related to the tumor response in HCC after TACE. The research confirmed that lipiodol, in addition to serving as a drug carrier and imaging tracer, can also function as an imaging biomarker for predicting tumor status after C-TACE.

Our team conducted the first CT radiomics study analyzing lipiodol deposits within TL post-initial TACE in 168 HCC (receiving ≥3 TACE sessions within six months), establishing these features—extracted from 24-hour post-TACE—as independent predictors of overall OS. The clinical-radiomic model demonstrated superior predictive performance compared to the radiomics model and clinical model alone. By extracting high-throughput CT radiomic features of lipiodol within the TL post-TACE, our study validates its potential value as an imaging biomarker. The key innovations of this work are as follows: first, this study addresses the limitation of low informational yield in non-contrast CT by utilizing lipiodol-retention patterns within TL—an innovative approach that not only distinguishes itself from previous studies[7–10,20,21] through direct characterization of tumor vascular permeability heterogeneity and intratumoral drug distribution dynamics, but also eliminates risks and financial burdens associated with contrast agent administration. Furthermore, in contrast to CT or MRI assessments conducted 1–3 months postoperatively, our method significantly advances the treatment response evaluation timeline to within 24 hours after TACE. This paradigm shift enables early identification of non-responders, preventing prolonged exposure to ineffective therapies and facilitating timely treatment optimization, including the integration of combined immunotherapy regimens.

Radiomics has been extensively utilized in various cancers, including lung cancer, breast cancer, and glioblastoma, for tasks such as tumor classification, prognosis prediction, and treatment response assessment.[22–24] These studies highlight the generalizability of radiomics in capturing tumor biology across different malignancies. Our study focuses on HCC, which presents unique challenges and opportunities for radiomics. Unlike cancers such as lung or breast cancer, where imaging interpretation is less affected by diffuse organ pathology, HCC often develops in the context of cirrhosis, introducing confounding factors such as background liver heterogeneity and variable contrast enhancement patterns. In HCC, lipiodol accumulation patterns of TL serve as dynamic biomarkers of post-embolization necrosis, while radiomics feature derived from these patterns capture prognostically significant intratumoral heterogeneity more effectively than static pretreatment imaging used in other malignancies. For instance, Original-ngtdm-Complexity reflects the consistency of cellular and tissue structure within tumors by quantifying the homogeneity of pixel value distribution in the VOI of medical images, representing the uniformity of tumor blood supply and metabolism. In our study, HCC lesions with lower complexity values exhibited more regular microvascular distribution, more homogeneous lipiodol deposits, and more thorough penetration of chemotherapeutic agents, indicating a better prognosis after TACE therapy. Moreover, Original-shape-Sphericity reflects tumor invasiveness and its relationship with surrounding tissues by quantifying the geometric features of the VOI. A lower sphericity ratio indicates infiltrative tumor growth, stronger invasive potential, and a higher likelihood of vascular invasion. Conversely, a higher ratio suggests well-defined, regular-shaped lipiodol-retention after TACE therapy, which are more likely to induce complete tumor necrosis and predict better prognosis in HCC.

The Six-and-twelve model evaluates tumor burden using tumor diameter and number and is currently the most classic prognostic model, particularly applicable to populations with HBV-related HCC. This study performed an external validation of the Six-and-twelve model on training and validation cohorts. The results showed the predictive performance of the Six-and-twelve model was comparable to that reported in its original study.[6] In contrast, the clinical-radiomics model proposed in our study incorporated a radiomics signature characterizing inter-patient tumor imaging heterogeneity. It outperformed the Six-and-twelve model in predicting patient OS and may serve as a complementary tool to existing clinical scores. Furthermore, this study categorizes patients into high-risk and low-risk groups using a clinical-radiomic model, revealing significant differences in OS between the groups. For high-risk patients, alternative treatment options such as surgical resection, radiofrequency ablation, or systemic therapy may be considered based on pre-surgical condition, or close post-TACE monitoring may be advised. The clinical-radiomics model is visualized through a nomogram, enabling clinicians to efficiently obtain predictive results, thus enhancing the model's practical applicability.

Tumor number and AFP as independent risk factors for predicting OS in HCC patients were identified by our research. The BCLC staging system has been widely recognized and recommended by multiple guidelines for prognostic and therapeutic stratification in HCC patients. Although some previous studies[7,10,17] have confirmed that BCLC staging and Child-Pugh classification serve as important prognostic indicators in HCC, our findings demonstrate that neither parameter serves as an independent risk factor for predicting OS. Additionally, several studies[19–21,25,26] have examined the relationship between laboratory indicators (such as AFP, ALP, HbsAg) and HCC prognosis. Notably, this study found that tumor number ($n > 3$) also constitute an independent risk factor for identifying responsive HCC. Multiple intrahepatic lesions can manifest as either multicentric origin of HCC or intrahepatic metastasis of HCC. We posit that smaller lesions within the liver or microlesions undetectable by imaging may not receive effective TACE embolization, potentially leading to poor TACE prognosis and impacting the patient's OS. In approx. 19.6% of patients additional degradable starch microspheres after the first C-TACE. We found that DEB-TACE procedures did not affect the survival time of patients. Future research will focus on the generalizability of lipiodol in combined therapies using multiple embolic materials.

This study has several limitations. Firstly, the sample size collected from three medical centers is relatively small, necessitating validation of the model in larger prospective studies. An external validation cohort could be incorporated in subsequent large-scale studies to enhance the model's robustness, and future studies should focus on prospective validation of the model in a multi-center setting. Additionally, integrating machine learning approaches may further refine predictive performance. Secondly, while the combination of Spearman's rank correlation test and LASSO regression analysis offers high efficiency and sparsity, it may exhibit reduced stability when numerous features are included in the model. Consequently, future research should explore alternative feature selection methods.

Conclusion

In summary, this study presents a novel clinical-radiomic model incorporating post-TACE lipiodol-retention as a prognostic biomarker for OS in HCC patients. The model demonstrates robust predictive performance, suggesting potential for clinical implementation in treatment planning. Future research should focus on prospective validation and external dataset replication to enhance generalizability.

Abbreviations

HCC, hepatocellular carcinoma; CT, computed tomography; MRI, magnetic resonance imaging; LASSO, least absolute shrinkage and selection operator; AUC, area under the curve; Rad-score, radiomics score; TL, target lesions; OS, overall survival; AFP, alpha-fetoprotein; C-TACE, conventional transarterial chemoembolization; DEB-TACE, drug-eluting beads transarterial chemoembolization; ROC, receiver operating characteristic; BCLC, stage of Barcelona Clinic Liver Cancer; HR, hazard ratio; CI, confidence interval; Tbil, TBIL, total bilirubin.

Ethics Approval and Informed Consent

This study was approved by the Institutional Review Board of The First Affiliated Hospital of Xinjiang Medical University. The need for informed consent was waived, and all methods were performed in accordance with the Declaration of Helsinki.

Author Contributions

All authors made a significant contribution to the work reported, whether that is in the conception, study design, execution, acquisition of data, analysis and interpretation, or in all these areas; took part in drafting, revising or critically reviewing the article; gave final approval of the version to be published; have agreed on the journal to which the article has been submitted; and agree to be accountable for all aspects of the work.

Funding

This work was supported by the Xinjiang Uygur Autonomous Region Natural Science Foundation Key Project (2021D01D22).

Disclosure

Han Yang and Juan Zhao are co-first authors for this study. The authors have no conflicts of interest in this work.

References

1. Sung H, Ferlay J, Siegel RL, et al. Global Cancer Statistics 2020: GLOBOCAN Estimates of Incidence and Mortality Worldwide for 36 Cancers in 185 Countries. *CA Cancer J Clin*. 2021;71(3):209–249. doi:10.3322/caac.21660
2. Vogel A, Cervantes A, Chau I, et al. Hepatocellular carcinoma: ESMO Clinical Practice Guidelines for diagnosis, treatment and follow-up. *Ann Oncol*. 2019;30(5):871–873. doi:10.1093/annonc/mdy308
3. Llovet JM, De Baere T, Kulik L, et al. Locoregional therapies in the era of molecular and immune treatments for hepatocellular carcinoma. *Nat Rev Gastroenterol Hepatol*. 2021;18(5):293–313. doi:10.1038/s41575-020-00395-0
4. Wu J, Liu W, Qiu X, et al. A Noninvasive Approach to Evaluate Tumor Immune Microenvironment and Predict Outcomes in Hepatocellular Carcinoma. *Phenomics*. 2023;3(6):549–564. doi:10.1007/s43657-023-00136-8
5. Wang XH, Fu YL, Xu YN, et al. Ginsenoside Rh1 regulates the immune microenvironment of hepatocellular carcinoma via the glucocorticoid receptor. *J Integr Med*. 2024;22(6):709–718. doi:10.1016/j.joim.2024.09.004
6. Wang Q, Xia D, Bai W, et al. Development of a prognostic score for recommended TACE candidates with hepatocellular carcinoma: a multicentre observational study. *J Hepatol*. 2019;70(5):893–903. doi:10.1016/j.jhep.2019.01.013
7. Cheng S, Hu G, Jin Z-Y, et al. CT-based radiomics nomogram for prediction of survival after transarterial chemoembolization with drug-eluting beads in patients with hepatocellular carcinoma and portal vein tumor thrombus. *Eur Radiol*. 2023;33(12):8715–8726. doi:10.1007/s00330-023-09830-7
8. Wang G, Ding F, Chen K, et al. CT-based radiomics nomogram to predict proliferative hepatocellular carcinoma and explore the tumor microenvironment. *J Transl Med*. 2024;22(1):683. doi:10.1186/s12967-024-05393-3
9. Ligero M, Garcia-Ruiz A, Viaplana C, et al. A CT-based Radiomics Signature Is Associated with Response to Immune Checkpoint Inhibitors in Advanced Solid Tumors. *Radiology*. 2021;299(1):109–119. doi:10.1148/radiol.2021200928
10. Ji G-W, Zhu F-P, Xu Q, et al. Radiomic Features at Contrast-enhanced CT Predict Recurrence in Early Stage Hepatocellular Carcinoma: a Multi-Institutional Study. *Radiology*. 2020;294(3):568–579. doi:10.1148/radiol.2020191470
11. Meng X-P, Wang Y-C, Ju S, et al. Radiomics Analysis on Multiphase Contrast-Enhanced CT: a Survival Prediction Tool in Patients With Hepatocellular Carcinoma Undergoing Transarterial Chemoembolization. *Front Oncol*. 2020;10:1196. doi:10.3389/fonc.2020.01196
12. Miszczuk MA, Chapiro J, Geschwind JH, et al. Lipiodol as an Imaging Biomarker of Tumor Response After Conventional Transarterial Chemoembolization: prospective Clinical Validation in Patients with Primary and Secondary Liver Cancer. *Transl Oncol*. 2020;13(3):100742. doi:10.1016/j.tranon.2020.01.003
13. Altman DG, Vergouwe Y, Royston P, et al. Prognosis and prognostic research: validating a prognostic model. *BMJ*. 2009;338(may28 1):b605. doi:10.1136/bmj.b605
14. European Association for the Study of the Liver. EASL Clinical Practice Guidelines: management of hepatocellular carcinoma. *J Hepatol*. 2018;69 (1):182–236. doi:10.1016/j.jhep.2018.03.019.
15. Zhong B, Zhang S, Zhu H, et al. Clinical Guidelines Committee of Chinese College of Interventionalists. Transarterial chemoembolization refractoriness in hepatocellular carcinoma: chinese College of Interventionalists definition and consensus statement. *Chin Med J*. 2024;137 (17):2040–2042. doi:10.1097/CM9.0000000000003109
16. Reig M, Forner A, Rimola J, et al. BCLC strategy for prognosis prediction and treatment recommendation: the 2022 update. *J Hepatol*. 2022;76 (3):681–693. doi:10.1016/j.jhep.2021.11.018
17. Fan W-Z, Zhu B-W, Chen S-L, et al. Survival in Patients With Recurrent Intermediate-Stage Hepatocellular Carcinoma: sorafenib Plus TACE vs TACE Alone Randomized Clinical Trial. *JAMA Oncol*. 2024;10(8):1047–1054. doi:10.1001/jamaoncol.2024.1831
18. Kong C-L, Zhao Z-W, Chen W-Y, et al. Prediction of tumor response via a pretreatment MRI radiomics-based nomogram in HCC treated with TACE. *Eur Radiol*. 2021;31(10):7500–7511. doi:10.1007/s00330-021-07910-0
19. Chen C-S, Li F-K, Guo C-Y, et al. Tumor vascularity and lipiodol deposition as early radiological markers for predicting risk of disease progression in patients with unresectable hepatocellular carcinoma after transarterial chemoembolization. *Oncotarget*. 2016;7(6):7241–7252. doi:10.18632/oncotarget.6892
20. Zhang K, Zhang L, Li W-C, et al. Radiomics nomogram for the prediction of microvascular invasion of HCC and patients' benefit from postoperative adjuvant TACE: a multi-center study. *Eur Radiol*. 2023;33(12):8936–8947. doi:10.1007/s00330-023-09824-5
21. Zhao Y, Zhang J, Wang N, et al. Intratumoral and peritumoral radiomics based on contrast-enhanced MRI for preoperatively predicting treatment response of transarterial chemoembolization in hepatocellular carcinoma. *BMC Cancer*. 2023;23(1):1026. doi:10.1186/s12885-023-11491-0
22. Liao C-Y, Chen Y-M, Wu Y-T, et al. Personalized prediction of immunotherapy response in lung cancer patients using advanced radiomics and deep learning. *Cancer Imaging*. 2024;24(1):129. doi:10.1186/s40644-024-00779-4
23. Wang X, Xie T, Luo J, et al. Radiomics predicts the prognosis of patients with locally advanced breast cancer by reflecting the heterogeneity of tumor cells and the tumor microenvironment. *Breast Cancer Res*. 2022;24(1):20. doi:10.1186/s13058-022-01516-0
24. Zhang Y, Zhang H, Zhang H, et al. Glioblastoma and Solitary Brain Metastasis: differentiation by Integrating Demographic-MRI and Deep-Learning Radiomics Signatures. *J Magn Reson Imaging*. 2024;60(3):909–920. doi:10.1002/jmri.29123
25. Jeong SO, Kim EB, Jeong SW, et al. Predictive Factors for Complete Response and Recurrence after Transarterial Chemoembolization in Hepatocellular Carcinoma. *Gut Liver*. 2017;11(3):409–416. doi:10.5009/gnl16001
26. Zheng B-H, Liu L-Z, Zhang -Z-Z, et al. Radiomics score: a potential prognostic imaging feature for postoperative survival of solitary HCC patients. *BMC Cancer*. 2018;18(1):1148. doi:10.1186/s12885-018-5024-z